Check for updates

Received: 13 April 2022 | Revised: 21 December 2022 | Accepted: 4 January 2023

DOI: 10.1002/hbm.26208

RESEARCH ARTICLE

WILEY

Disentangling poststroke cognitive deficits and their neuroanatomical correlates through combined multivariable and multioutcome lesion-symptom mapping

Nick A. Weaver[1] | Muhammad Hasnain Mamdani[2] | Jae-Sung Lim[3] | Johannes Matthijs Biesbroek[1] | Geert Jan Biessels[1] | Irene M. C. Huenges Wajer[1,4] | Yeonwook Kang[5,6] | Beom Joon Kim[7] | Byung-Chul Lee[5] | Keon-Joo Lee[8] | Kyung-Ho Yu[5] | Hee-Joon Bae[7] | Danilo Bzdok[2,9] | Hugo J. Kuijf[10]

[1]Department of Neurology and Neurosurgery, UMC Utrecht Brain Center, Utrecht, The Netherlands

[2]Department of Biomedical Engineering, Faculty of Medicine, McConnell Brain Imaging Centre, School of Computer Science, Montreal Neurological Institute (MNI), McGill University, Montreal, Canada

[3]Department of Neurology, Asan Medical Center, University of Ulsan College of Medicine, Seoul, Republic of Korea

[4]Experimental Psychology, Helmholtz Institute, Utrecht University, Utrecht, The Netherlands

[5]Department of Neurology, Hallym University Sacred Heart Hospital, Hallym Neurological Institute, Hallym University College of Medicine, Anyang, Republic of Korea

[6]Department of Psychology, Hallym University, Chuncheon, Republic of Korea

[7]Department of Neurology, Seoul National University Bundang Hospital, Seoul National University College of Medicine, Seongnam, Republic of Korea

[8]Department of Neurology, Korea University Guro Hospital, Seoul, Republic of Korea

[9]Mila—Quebec Artificial Intelligence Institute, Montreal, Canada

[10]Image Sciences Institute, University Medical Center Utrecht, Utrecht, The Netherlands

Correspondence
Nick A. Weaver, Department of Neurology and Neurosurgery, UMC Utrecht Brain Center, Utrecht, The Netherlands.
Email: n.a.weaver@umcutrecht.nl

Funding information
ZonMw, Grant/Award Number: 918.16.616; UMC Utrecht Brain Center; Brain Canada Foundation; Health Canada, National Institutes of Health, Grant/Award Numbers: NIH R01 R01DA053301-01A1, NIH R01 AG068563A; Canadian Institute of Health Research (CHIR), Grant/Award Numbers: CIHR 470425, CIHR 438531; Healthy Brains Healthy Lives initiative (Canada First Research Excellence fund; Google (Research Award, Teaching Award); CIFAR Artificial Intelligence Chairs program (Canada Institute for Advanced Research); Dutch Heart Foundation, Grant/Award

Abstract

Studies in patients with brain lesions play a fundamental role in unraveling the brain's functional anatomy. Lesion-symptom mapping (LSM) techniques can relate lesion location to cognitive performance. However, a limitation of current LSM approaches is that they can only evaluate one cognitive outcome at a time, without considering interdependencies between different cognitive tests. To overcome this challenge, we implemented canonical correlation analysis (CCA) as combined multivariable and multioutcome LSM approach. We performed a proof-of-concept study on 1075 patients with acute ischemic stroke to explore whether addition of CCA to a multivariable single-outcome LSM approach (support vector regression) could identify infarct locations associated with deficits in three well-defined verbal memory functions (encoding, consolidation, retrieval) based on four verbal memory subscores derived from the Seoul Verbal Learning Test (immediate recall, delayed recall, recognition, learning

Danilo Bzdok and Hugo J. Kuijf contributed equally to this study.

This is an open access article under the terms of the Creative Commons Attribution-NonCommercial License, which permits use, distribution and reproduction in any medium, provided the original work is properly cited and is not used for commercial purposes.
© 2023 The Authors. *Human Brain Mapping* published by Wiley Periodicals LLC.

Number: 03-004-2021-T043

ability). We evaluated whether CCA could extract cognitive score patterns that matched prior knowledge of these verbal memory functions, and if these patterns could be linked to more specific infarct locations than through single-outcome LSM alone. Two of the canonical modes identified with CCA showed distinct cognitive patterns that matched prior knowledge on encoding and consolidation. In addition, CCA revealed that each canonical mode was linked to a distinct infarct pattern, while with multivariable single-outcome LSM individual verbal memory subscores were associated with largely overlapping patterns. In conclusion, our findings demonstrate that CCA can complement single-outcome LSM techniques to help disentangle cognitive functions and their neuroanatomical correlates.

KEYWORDS

canonical correlation analysis, cognitive impairment, ischemic stroke, lesion location, lesion-symptom mapping, pattern-learning algorithms, support vector regression, verbal memory

1 | INTRODUCTION

Studies in patients with brain lesions are fundamental to the understanding of the functional architecture of the brain (Karnath et al., 2018; Rorden & Karnath, 2004). This is based on the principle that if a particular function is impaired in a patient with a lesion, this function can be ascribed to the location of this lesion. Throughout the past two decades, lesion-symptom mapping (LSM) techniques have become increasingly popular to relate brain lesion locations to behavioral measures such as cognition (de Haan & Karnath, 2017). This is commonly done through statistical comparisons of patients with and without a lesion for individual voxels or by associating regional lesion volumes with cognitive scores.

Traditional LSM techniques, most notably voxel-based LSM (VLSM; Bates et al., 2003; Rorden et al., 2007), are univariable (i.e., analyzing each voxel or brain region separately) and univariate (i.e., analyzing a single outcome or clinical endpoint at a time). This analytical approach seems straightforward, but there are two important pitfalls. First, brain regions are anatomically linked and can thus be systematically damaged together. For example, brain infarcts do not occur randomly, but follow the vascular topography of the brain. Second, neuropsychological tests generally rely on multiple cognitive functions. Not all of these functions are directly related to the primary function that a test aims to probe. For example, most tests depend on verbal or written instructions and thus partially rely on language abilities. Hence, when test scores correlate with each other, this commonality does not necessarily represent the cognitive function that the test aims to probe, but can also represent other shared components. Therefore, both the cross-dependencies between lesion locations and cognitive performance dimensions (i.e., commonly multiple test scores) should be taken into account to avoid falsely attributing a function to a particular location.

The interdependency between lesion locations is a topic of increasing interest, and various multivariable LSM techniques have been developed to address this issue (e.g., Mirman et al., 2017; Pustina et al., 2017; Wilson et al., 2010; Zhang et al., 2014; Zhao et al., 2017). Meanwhile, the interdependency between cognitive scores is commonly dealt with by consecutively analyzing multiple cognitive tests that depend on shared and distinct cognitive functions in separate univariate analyses (Sperber et al., 2020). Shared and distinct anatomical correlates are then ascribed to the shared and distinct cognitive functions through indirect comparisons of these separate analyses (e.g., in Biesbroek et al., 2016, 2021). However, there are methodological challenges to this approach, given that the complex interrelationship between cognitive tests is not taken into account and the comparison between the different analyses is generally qualitative (illustrated in Figure 1). Indeed, a recent study demonstrated that this approach can lead to topographical bias and false-positive artifacts (Sperber et al., 2020). To our knowledge, thus far no suitable solution to this issue has been proposed. Multioutcome modeling strategies could potentially overcome this. From a theoretical perspective, canonical correlation analysis (CCA) is a promising candidate for multioutcome LSM (Hotelling, 1936; Wang et al., 2020). CCA can simultaneously evaluate two different sets of variables (e.g., a set of cognitive scores and a set of measures for brain infarct location), thereby taking the interrelationship within a set of variables (e.g., cognitive scores related to each other) and between sets of variables (e.g., cognitive scores related to infarct locations) into account in a single model (Bzdok et al., 2019; Clemens et al., 2020; Wang et al., 2020). These statistical properties could be advantageous for LSM analyses, because CCA can account for both the interrelationship between infarct locations (i.e., similar to available multivariable LSM techniques) and the interrelationship between cognitive scores at the same time. Of note, a form of CCA has been previously implemented in LSM, but only as multivariable approach to increase spatial accuracy and reliability of results, and not to address multiple outcomes simultaneously (Pustina et al., 2017).

Here, we performed a proof-of-concept study on 1075 patients with acute ischemic stroke, in which we evaluated whether addition of CCA to a multivariable single-outcome LSM analysis pipeline could aid identification of infarct locations related to specific cognitive functions. For this purpose, we examined three commonly used and well-defined verbal memory functions as outcomes of interest: encoding,

10970193, 2023, 6, Downloaded from https://onlinelibrary.wiley.com/doi/10.1002/hbm.26208 by Utrecht University Library, Wiley Online Library on [11/05/2023]. See the Terms and Conditions (https://onlinelibrary.wiley.com/terms-and-conditions) on Wiley Online Library for rules of use; OA articles are governed by the applicable Creative Commons License

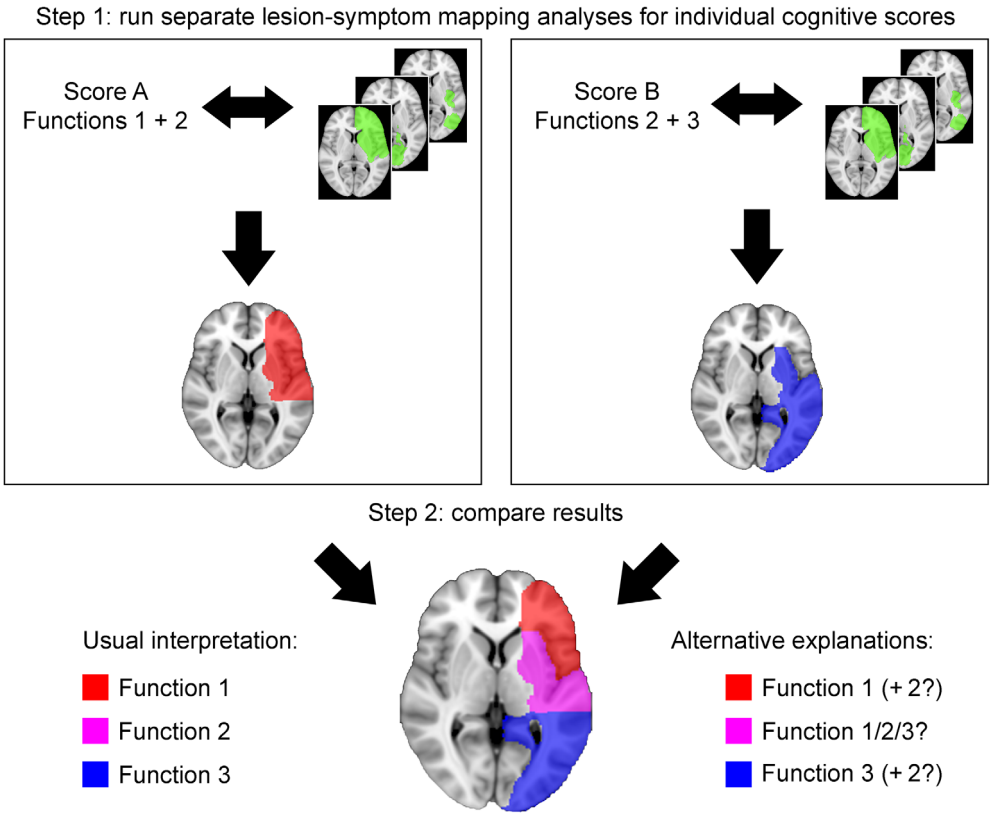

FIGURE 1 Conventional approach to inferring the neural correlates of cognitive functions from single-outcome lesion-symptom mapping. Cognitive tests generally encompass multiple cognitive functions. In this hypothetical example, test Score A encompasses Functions 1 and 2, and Score B Functions 2 and 3. This means that scores reflect partially overlapping and partially distinct functions. For example, Scores A and B both measure Function 2, whereas score A measures Function 1 but Score B does not. In LSM Scores A and B are analyzed separately, and relevant lesion locations are revealed for each score. Results can be plotted and compared visually (shown here in red and blue in the upper panel). The left side of the lower panel shows the usual interpretation of such results, in which overlapping locations (shown in purple) are assigned to functions that are shared between the two scores, in this example Function 2, and the nonoverlapping locations to functions that differ between the scores (Function 1 for Score A, Function 3 for B). The right side of the lower panel demonstrates alternative explanations that are also compatible with the lesion distributions for Scores A and B. Single-outcome LSM is not able to identify which explanation is correct.

consolidation, and retrieval (Baddeley & Hitch, 1974). We used the Seoul Verbal Learning Test (SVLT) as cognitive assessment, from which we selected four verbal memory subscores. We explored: (1) whether CCA could extract cognitive patterns that represent verbal memory functions, by comparing the cognitive patterns derived from the subscores to prior theoretical knowledge; and (2) to what extent CCA could link the identified cognitive patterns to more specific infarct locations than single-outcome LSM alone.

2 | MATERIALS AND METHODS

2.1 | Study population

Patients were selected from the Hallym Vascular Cognitive Impairment (VCI) and Bundang VCI cohorts, consisting of patients admitted to Hallym University Sacred Heart Hospital or Seoul National University Bundang Hospital (Republic of Korea) with acute ischemic stroke between January 2007 and December 2018 (Lim et al., 2014; Yu et al., 2013). A total of 1075 patients were eligible for the present investigation based on the following inclusion criteria: (1) brain magnetic resonance imaging (MRI) showing the acute symptomatic infarct(s) on diffusion-weighted imaging (DWI) and/or fluid-attenuated inversion recovery (FLAIR), (2) successful infarct segmentation and registration (Section 2.2), (3) no previous cortical infarcts, large subcortical infarcts or intracerebral hemorrhages on MRI (Section 2.2), and (4) available SVLT assessment that includes all four cognitive scores (Section 2.3) and clinical data on age, sex, and education. At the discretion of the attending physician, patients were not included in the study if they suffered from disabilities that would interfere with neuropsychological testing, including neurological deficits such as severe aphasia or severe motor weakness, or impairment of hearing or vision. A flowchart of patient selection is provided in Figure 2.

2.2 | Generation of lesion maps

Lesion data were available from a previous project (Weaver et al., 2021). In short, infarct segmentation and subsequent registration to the T1 MNI-152 brain template (resolution 1 × 1 × 1 mm;

10970193, 2023, 6, Downloaded from https://onlinelibrary.wiley.com/doi/10.1002/hbm.26208 by Utrecht University Library, Wiley Online Library on [11/05/2023]. See the Terms and Conditions (https://onlinelibrary.wiley.com/terms-and-conditions) on Wiley Online Library for rules of use; OA articles are governed by the applicable Creative Commons License

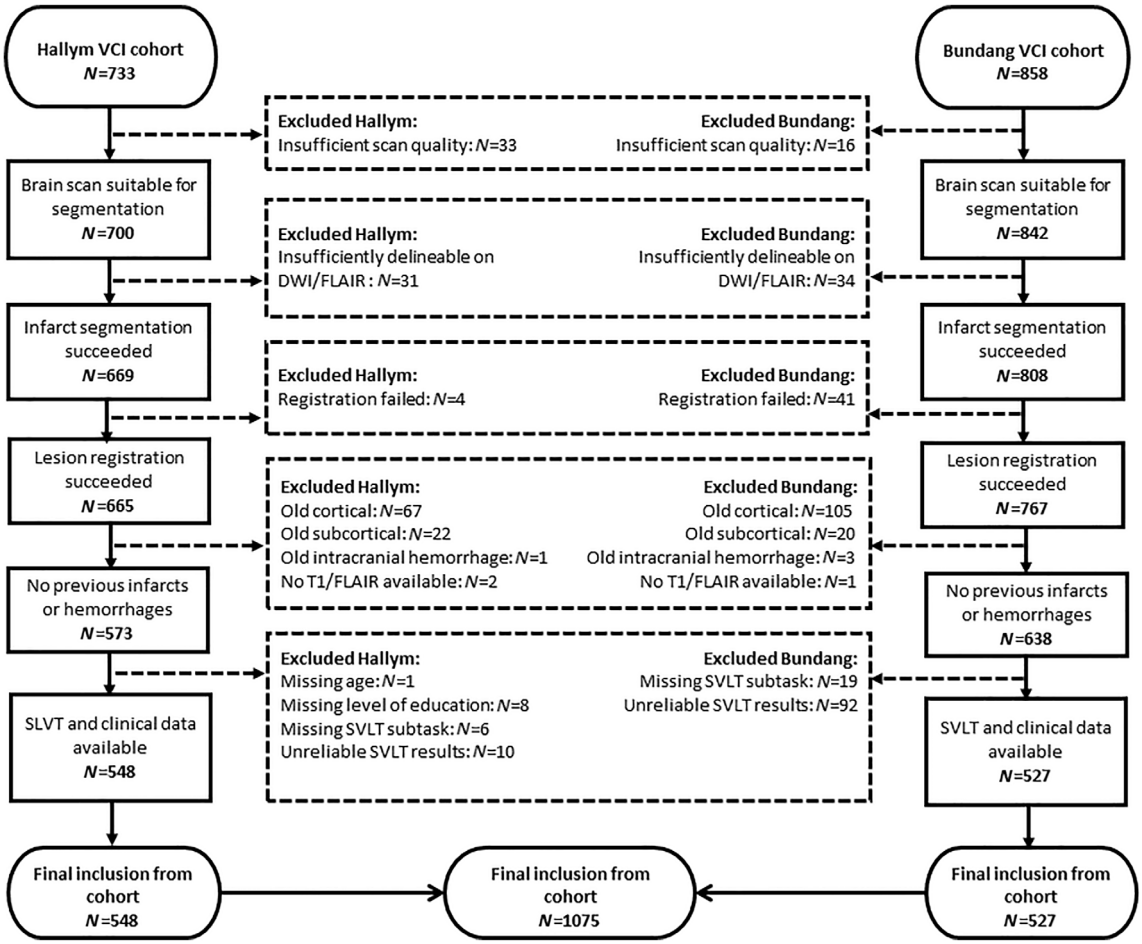

FIGURE 2 Flowchart of patient selection. Seoul Verbal Learning Test (SVLT) results were deemed unreliable if the recognition subscore was <12 (maximum: 24), because that would mean that patients performed worse than chance level. Availability of all four SVLT subscores (i.e., immediate recall, delayed recall, recognition, and learning ability) was required for inclusion in this study.

Fonov et al., 2011) were performed in accordance with a previously published protocol (Biesbroek et al., 2019). First, acute infarcts were manually segmented on DWI ($N = 1048$; 97.5%) or FLAIR ($N = 27$; 2.5%) sequences using in-house developed software built in MeVisLab (MeVis Medical Solutions AG, Bremen, Germany; Ritter et al., 2011). ADC and T1 sequences were used as reference when available. Next, all scans and the corresponding lesion maps were transformed to MNI-152 space with the RegLSM tool (https://github.com/Meta-VCI-Map/RegLSM). Quality checks of all registration results were performed by an experienced rater (Nick A. Weaver) and manual adaptations were made in case of minor registration errors ($N = 468$; 43.5%). Presence of chronic cortical infarcts (any size), large subcortical infarcts (>15 mm), and large intracerebral hemorrhages (>10 mm) was assessed by an experienced rater (Nick A. Weaver), and patients with any of these lesions were excluded from this study.

2.3 | Neuropsychological assessment

Four verbal memory subscores derived from the SVLT were used for the present study. The SVLT is a verbal memory test that consists of a list of 12 nouns with four words drawn from each of three semantic categories: flowers, writing materials, and kitchen appliances (Kang & Na, 2003). The SVLT includes three learning trials, a 20-min delayed recall trial, and a yes/no delayed recognition trial. The recognition trial consists of a randomized list of 12 target and 12 nontarget words, six of which are drawn from the same categories as those of the targets. Three scores were directly taken from the SVLT test battery: immediate recall (i.e., sum of all three trials), delayed recall, and recognition. A fourth subscore, for learning ability, was calculated by taking the increase in number of words remembered between the first and last learning trial. Patients with a recognition score below 12 (maximum: 24) were excluded (see Figure 2), because it was deemed improbable that this task performance was worse than chance level. All four SVLT subscores were converted into sample-based z-scores and individually adjusted for age, sex, education level, and total infarct volume using linear regression. Recognition subscores were natural log-transformed to fit the linearity requirements of the feature selection step of the support vector regression (SVR) analyses.

Three verbal memory functions are distinguished in Baddeley's model for memory: encoding, consolidation, and retrieval (Baddeley & Hitch, 1974). Based on this model, combinations of findings on

10970193, 2023, 6, Downloaded from https://onlinelibrary.wiley.com/doi/10.1002/hbm.26208 by Utrecht University Library, Wiley Online Library on [11/05/2023]. See the Terms and Conditions (https://onlinelibrary.wiley.com/terms-and-conditions) on Wiley Online Library for rules of use; OA articles are governed by the applicable Creative Commons License

different SVLT subscores were hypothesized to represent different verbal memory functional deficits. Hypothesized patterns of subscores that would represent each of the verbal memory functions are shown in Table 1. Impaired learning ability subscores suggest an encoding deficit. Immediate recall subscores also capture information on encoding, but are less specific. Immediate and delayed recall can also be impaired as downstream effect, as retrieval is not possible without prior encoding. The combination of impaired delayed recall and impaired recognition subscores suggests a consolidation deficit, but only if learning ability and immediate recall subscores are relatively unimpaired. An impaired delayed recall subscore combined with a relatively unimpaired recognition subscore suggests a retrieval deficit.

2.4 | Machine learning analysis workflow

We implemented a two-step analysis approach. As first analysis step, we performed SVR region of interest (ROI)-based LSM (SVR-ROI), which is a well-established multivariable LSM method (Zhang et al., 2014; Zhao et al., 2017). SVR-ROI was done for each SVLT subscore individually. As second analysis step, we selected ROIs that were statistically significant in one or more individual SVR-ROI analyses for the CCA analysis. A schematic overview is shown in Figure 3, and details on SVR-ROI and CCA analysis steps are described below.

This two-step approach was applied to deal with the directionality of lesion-symptom associations. In LSM, coefficients are calculated based on within-group comparisons, meaning that they represent the relative performance between patients, and are not compared to healthy controls. All included patients have a brain lesion, and some will perform worse than others on cognitive tests. Negative coefficients—that is, when damage to a particular region is associated with better cognitive performance—represent relatively good performance within the patient group. Therefore, only positive coefficients are considered relevant from a clinical perspective in LSM. With traditional LSM techniques such as VLSM and SVR-based LSM, a coefficient is calculated for each location (i.e., voxel/region) separately, allowing negative coefficients to be filtered out post hoc. Meanwhile, CCA inherently creates the canonical modes based on strength of both positive and negative coefficients (i.e., weights). This means that each mode is still driven by both positive and negative correlations, making it difficult to interpret the resulting association patterns. For this reason, we performed CCA as secondary step following SVR-ROI. SVR-ROI allowed us to first identify ROIs with positive coefficients for verbal memory functions, and subsequently only enter these ROIs in the CCA to reduce the effect of negative coefficients when creating the canonical modes.

2.4.1 | SVR step

SVR-ROI was performed using MATLAB (version R2018a), in accordance with previously published methods (Zhao et al., 2017). Regional infarct volumes of a total of 163 predefined ROIs were used as input variables for the SVR-ROI. These volumes were calculated in milliliters in MNI-152 1 mm space (Fonov et al., 2011) using the Harvard-Oxford grey matter atlas (111 ROIs; Makris et al., 2006), ICBM DTI-81 white matter atlas (50 ROIs; Mori et al., 2008), and the Hammers atlas for the cerebellar hemispheres (2 ROIs; Hammers et al., 2003). Only ROIs damaged in at least five patients were included in the analyses. A linear SVR model with feature selection was used (Yourganov et al., 2016). In the feature selection step, ROIs with a univariate significant Pearson correlation ($p < .05$) between infarct volume and SVLT subscores were selected. Parameter training of the linear SVR model was performed to determine the optimal regularization parameter (C) to maximize the prediction performance. Prediction performance was calculated for each C by determining the mean Pearson correlation coefficient between the real and predicted SVLT subscores with 5-fold cross-validations (optimal parameters in Table S1). Statistical inference was performed by shuffling the observations of z-scores to create pseudoweight coefficients. The significance level of each voxel was calculated by counting the number of pseudoweights larger than the real weight in 5000 permutations. ROIs with permutation-based $p < .05$ were considered statistically significant.

2.4.2 | Multivariable multioutcome cross-association step

CCA identifies sources of common variation in two sets of variables, in our case regional infarct volumes and SVLT subscores. Joint

TABLE 1 Theoretical constructs for verbal memory functions and representation by Seoul Verbal Learning Test subscores

Function	Definition	Score impaired in case of functional deficit?			
		Immediate recall	Delayed recall	Recognition	Learning ability
Encoding	Ability to attend to and register new information	Possibly[a]	Possibly[a]	Yes	Yes
Consolidation	Ability to maintain, elaborate, and store new information in long-term memory	No	Yes	Yes	Yes, but less specific than delayed recall and recognition
Retrieval	Ability to retrieve information from long-term memory	Yes, but less specific than delayed recall	Yes	No	No

[a]Impaired as downstream effect, because words cannot be recalled if the words are not encoded (Lezak et al., 2012; Vanderploeg et al., 2001).

10970193, 2023, 6, Downloaded from https://onlinelibrary.wiley.com/doi/10.1002/hbm.26208 by Utrecht University Library, Wiley Online Library on [11/05/2023]. See the Terms and Conditions (https://onlinelibrary.wiley.com/terms-and-conditions) on Wiley Online Library for rules of use; OA articles are governed by the applicable Creative Commons License

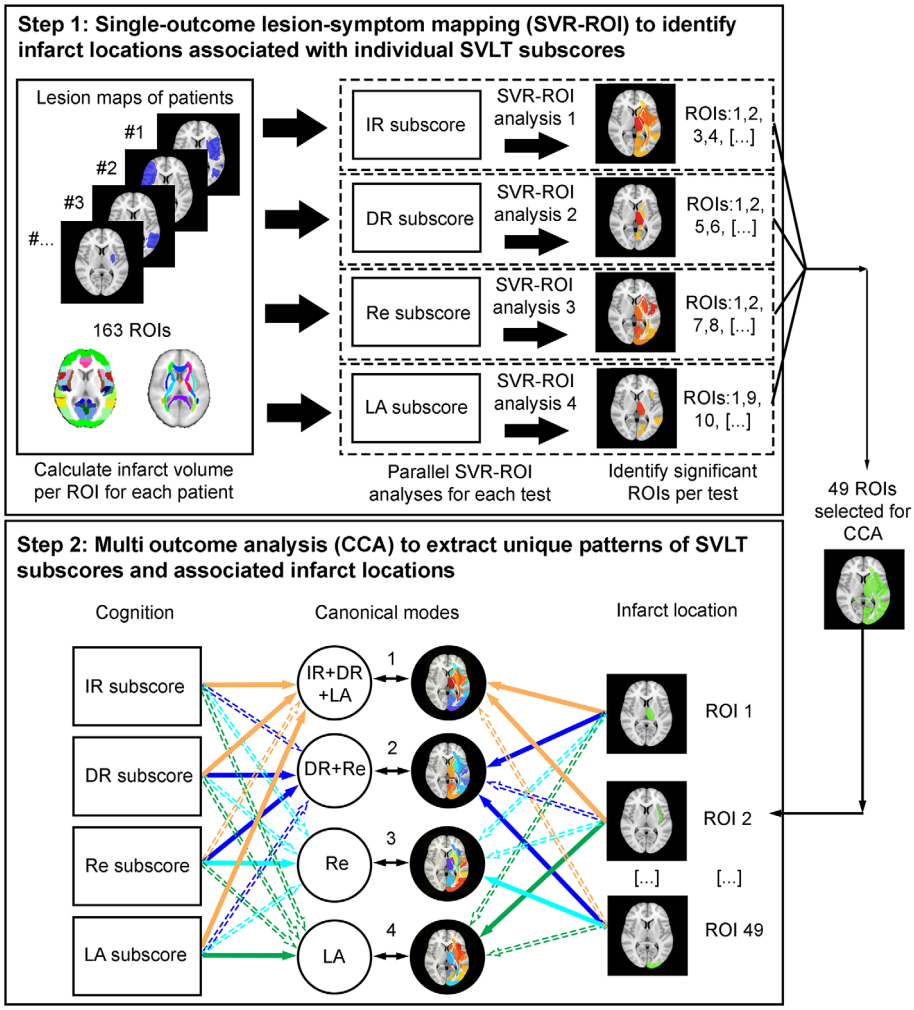

FIGURE 3 Schematic overview of analysis steps. An overview of the analysis steps is shown, using actual data from present study. Prior to analyses, infarct volumes in predefined regions of interest (ROIs) were calculated for each patient. In Step 1, we performed support vector regression-based lesion-symptom mapping (SVR-ROI), in which the association between ROI infarct volumes and four Seoul Verbal Learning Test (SVLT) subscores was analyzed individually across all 163 ROIs. This resulted in the identification of ROIs where infarct volumes were significantly associated with one or more SVLT subscores (upper right panel; corresponding with Figure 4). Only the 49 ROIs with a significant association in the SVR-ROI for one or more subscores ($p < .05$, 5000 permutations) were selected for the subsequent canonical correlation analysis (CCA) analysis. In Step 2, the 49 selected ROIs and all SVLT subscores were entered in a single CCA model. Four canonical modes were produced (i.e., equal to the minimum number of cognitive variables, in this case SVLT subscores, entered in the model) using a purely data-driven approach. Each canonical mode represented a unique pattern of paired cognitive (white circles) and lesion data (black circles). For each mode, positive betas on both the SVLT subscore (here only the name of associated subscore per mode is given; see Figure 5 for full results) and ROIs (colors yellow to red) indicate that poorer performance on the SVLT subscore(s) is linked to higher infarct volumes Arrows indicate whether or not the test or ROI contributed to a mode; filled arrows indicate a strong contribution, dashed arrows indicate little or no contribution (corresponding with neutral or negative betas). DR, delayed recall; IR, immediate recall; LA, learning ability; Re, recognition.

modeling of SVLT subscores exploits the existence of shared underlying processes between various cognitive functions to model brain-behavior relationships. CCA, similar to Principal Component Analysis, performs change of basis, but of both sets of variables simultaneously. It does so by transforming both sets of variables to latent space such that linear correspondence between each corresponding latent dimension is maximized (Wang et al., 2020). More details are presented below.

Mathematical notions

Let, $\boldsymbol{X}$ and $\boldsymbol{Y}$ are two sets of variables with dimensions p and q, respectively. The first CCA mode estimates the parameters associated with canonical vectors a and b from each set of variables as follows:

$$U = a^T \boldsymbol{X}; a \in R^p$$

$$V = b^T \boldsymbol{Y}; b \in R^q$$

10970193, 2023, 6, Downloaded from https://onlinelibrary.wiley.com/doi/10.1002/hbm.26208 by Utrecht University Library, Wiley Online Library on [11/05/2023]. See the Terms and Conditions (https://onlinelibrary.wiley.com/terms-and-conditions) on Wiley Online Library for rules of use; OA articles are governed by the applicable Creative Commons License

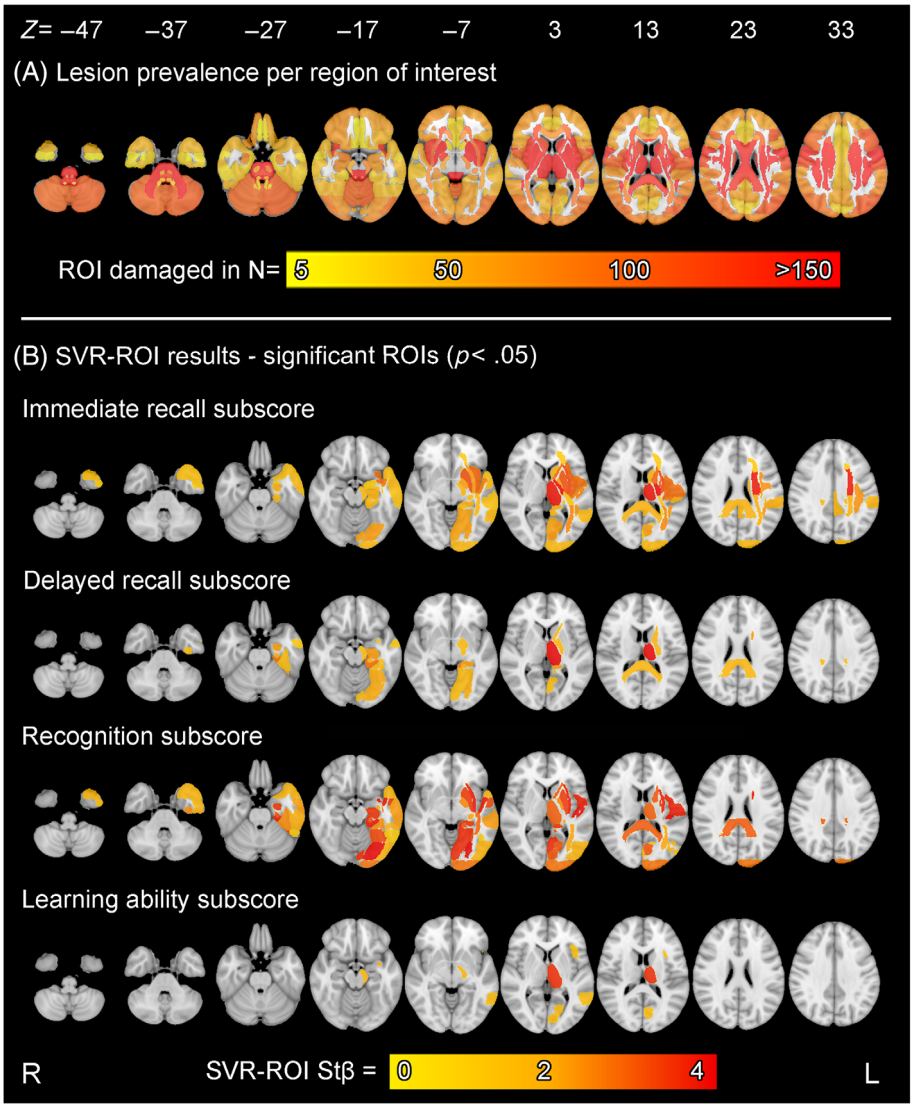

FIGURE 4 Lesion prevalence and single-outcome support vector regression (SVR) region of interest (ROI)-based lesion-symptom mapping (SVR-ROI) results. (A) Infarct prevalence map showing ROIs that are damaged in ≥5 patients (total $N = 1075$) and thus included in the SVR-ROI analyses. (B) Results of region of interest-based lesion-symptom mapping (SVR-ROI) for each cognitive test. ROIs were defined by the Harvard-Oxford gray matter atlas, ICBM DTI-81 white matter atlas, and the Hammers atlas for the cerebellar hemispheres. ROIs from the SVR-ROI analysis are shown ($p < .05$; based on 5000 permutation iterations); colors indicate the standardized beta for each ROI (i.e., higher betas indicate that higher infarct volume is associated with worse cognitive performance). L, left; R, right; Stβ, standardized beta.

such that the linear association as measured by Pearson correlation between U and V, the canonical variates, is maximized.

$$\rho = \mathrm{corr}\,(U,V) = \mathrm{corr}\left(a^T\boldsymbol{X}, b^T\boldsymbol{Y}\right).$$

Here, ρ represents the canonical correlation.

Canonical Modes 2, 3, and so on up to min (p, q) can also be obtain in a similar way with the condition that canonical modes are uncorrelated with each other.

Region of interest-based analyses using CCA were performed using the Python 3.7 environment using the packages Scikit-learn (version 0.22.1; Abraham et al., 2014) and Nilearn (version 0.5.2; Pedregosa et al., 2011). The code is publicly available at: https://github.com/hasnainmamdani/stroke-impairment-inference-lsm-cca/. Infarct volumes in the predefined ROIs were the same as used in the SVR-ROI analyses.

Infarct volumes of the 49 statistically significant ROIs obtained from the SVR-ROI analysis were z-transformed and fed to the CCA model, on the one hand, along with all four SVLT subscores, on the other hand. Four canonical modes were extracted, equal to the minimum number of variables in either of the variable sets (in this case, SVLT subscores; Wang et al., 2020). Canonical vectors were obtained that represent the contribution of every brain region and SVLT subscore for each mode. The explained variance for each canonical mode was calculated as the Pearson correlation between the corresponding canonical variates (of infarct volumes of ROIs and SVLT subscores) of each mode. We evaluated whether CCA could extract patterns of SVLT subscores that match prior theoretical knowledge of verbal memory functions, by comparing the SVLT subscore patterns from the canonical modes to the hypothesized representations of cognitive functions, as shown in Table 1. For each canonical mode, p-values per ROI were calculated using random permutation testing (1000 permutations). Z-scores of the four SVLT subscores were shuffled independently in each permutation and CCA was fitted on the permuted data to obtain pseudocanonical vectors. The significance level of each ROI was calculated by counting the number of times the pseudoweights associated with each ROI and canonical mode were larger (smaller for

10970193, 2023, 6, Downloaded from https://onlinelibrary.wiley.com/doi/10.1002/hbm.26208 by Utrecht University Library, Wiley Online Library on [11/05/2023]. See the Terms and Conditions (https://onlinelibrary.wiley.com/terms-and-conditions) on Wiley Online Library for rules of use; OA articles are governed by the applicable Creative Commons License

negative weights) than the original weight in 1000 permutations. To take the analysis of 49 ROIs into account, correction for multiple comparisons was performed by repeating random permutation testing using 49,000 iterations (i.e., 49 × 1000). As additional step, CCA was repeated without correction for total infarct volume, to determine whether this correction had any impact on the results.

3 | RESULTS

3.1 | Study population

Demographic and clinical characteristics of 1075 included patients are provided in Table 2. Mean age was 67 years (SD = 12), 452 patients were female (42%), and median years of education was 9 (interquartile range [IQR] = 6–12). Infarcts were generally small, with a median normalized volume of 2.3 ml (IQR = 0.9–12.3). SVLT assessment most commonly took place 3–4 months poststroke, with a median of 98 days (IQR = 84–125). SVLT subscores covered the full range of possible scores, and included substantial numbers of patients with clinically relevant impairment (i.e., scores <3rd percentile based on age-corrected and education-corrected local normative data: for immediate recall 22% of patients, delayed recall 22%, and recognition subscores 25%; Table 2). No normative data were available for learning ability.

TABLE 2 Demographic and clinical characteristics of study sample ($N = 1075$).

Demographics and clinical characteristics	Total sample ($N = 1075$)
Age (years), mean (SD)	66.5 (11.7)
Female, *N* (%)	452 (42.0%)
Years of education, median (IQR)	9 (6–12)
Hand preference, *N* (%)	(Missing $N = 19$)
Right	1033 (97.8%)
Left	9 (0.9%)
Ambidextrous	14 (1.3%)
Verbal memory assessment	
Time interval between stroke onset and assessment (days), median (IQR), range	98 (84–125), range 1–365 (missing $N = 3$)
Immediate recall (sum of 3 trials, max. range 0–36), median (IQR), range	16 (12–20), range 0–36
Immediate recall, impaired based on normative data (<3rd percentile), *N* (%)[a]	235 (22.0%; missing $N = 5$)
Delayed recall (maximum range 0–12), median (IQR), range	4 (2–6), range 0–12
Delayed recall, impaired based on normative data (<3rd percentile), *N* (%)[a]	240 (22.4%; missing $N = 2$)
Recognition (maximum range 0–24), median (IQR), range	20 (17–22), range 0–24
Recognition, impaired based on normative data (<3rd percentile), *N* (%)[a]	261 (24.5%; missing $N = 10$)
Learning ability (difference immediate recall trials 1–3), median (IQR), range[b]	3 (2–4), range 0–9
Brain MRI	
Time interval between stroke onset and MRI (days), median (IQR), range	3 (1–5), range 0–46
Total infarct volume in ml,[c] median (IQR), range	2.3 (0.9–12.3), range 0.04–535.1

Note: Missing data are noted behind the respective variable, when appropriate. Valid percent is indicated in cases with missing data.
Abbreviations: IQR, interquartile range; MRI, magnetic resonance imaging; SD, standard deviation.
[a]Percentile scores were calculated using local normative data from a healthy population-based sample (Kang and Na, 2003).
[b]No normative data available for learning ability score.
[c]Normalized volumes after registration to the MNI-152 template.

3.2 | Lesion prevalence and brain coverage

Lesion prevalence per region of interest is shown in Figure 4a. Infarct distribution was symmetrical and subcortical regions were more commonly damaged than cortical regions. Overall brain lesion coverage was high: all 163 ROIs were damaged in at least 5 patients and therefore included in the SVR-ROI analyses.

3.3 | SVR-ROI results

Forty-nine ROIs were significantly associated ($p < .05$, 5000 permutations) with one or more SVLT subscores (Figure 4b and Table S2). All significant ROIs were located in the left hemisphere, except for the corpus callosum ROI that crossed between both hemispheres. Each verbal memory subscore was significantly associated with multiple ROIs. Immediate recall and recognition subscores were both associated with infarct volumes in an extensive pattern of ROIs, with a large degree of ROI overlap between subscores. Delayed recall and learning ability subscores were associated with fewer ROIs, but these ROIs largely overlapped with those associated with immediate recall and recognition scores. Of note, very few ROIs were associated with only a single SVLT subscore: immediate recall subscores were exclusively associated with infarct volumes in the left subcortical white matter, recognition subscores were exclusively associated with infarct volumes in left temporo-occipital gyri, and learning ability subscores were exclusively associated with infarct volumes in the left frontal operculum cortex. Delayed recall subscores had no exclusive associations. All four SVLT subscores showed high betas in the thalamus; immediate recall and recognition showed high betas in the basal ganglia, medial temporal lobe, occipital lobe, and frontoparietal ROIs. Delayed recall and learning ability only showed high betas for the thalamus.

We translated the SVR-ROI results for individual SVLT subscores back to the theoretical constructs of verbal memory functions using Table 1 as framework. Next, we evaluated the spatial patterns of

10970193, 2023, 6, Downloaded from https://onlinelibrary.wiley.com/doi/10.1002/hbm.26208 by Utrecht University Library, Wiley Online Library on [11/05/2023]. See the Terms and Conditions (https://onlinelibrary.wiley.com/terms-and-conditions) on Wiley Online Library for rules of use; OA articles are governed by the applicable Creative Commons License

overlap and difference between significant ROIs as shown in Figure 4b. The interpretation for consolidation and retrieval is illustrated in Figure 5. Two ROIs in the temporo-occipital fusiform cortex fit the theoretical construct for consolidation, whereas no ROIs fit the pattern for retrieval. For encoding, impairment in any of the four SVLT subscores could theoretically result in an encoding deficit, therefore we could not extract ROIs by comparing individual SVLT subscore results to the theoretical construct without taking their relative contribution into account.

3.4 | CCA results

The 49 ROIs selected with the SVR-ROI and all four SVLT subscores were entered in the CCA model, and four canonical modes were extracted. CCA results are shown in Figure 6 and Tables S3 and S4. Table S4 shows the *p*-values per ROI calculated through random permutation testing. Cognitive scores in Mode 1 were primarily driven by immediate and delayed recall subscores (i.e., high weights compared to the other SVLT subscores), and lower scores were most strongly associated with higher infarct volumes in the left thalamus (Figure 6). Mode 2 was driven by delayed recall and recognition subscores, and to lesser extent learning ability subscores, and lower scores were most strongly associated with higher infarct volumes in the left occipital and medial temporal lobes including the hippocampus. Mode 3 was driven by recognition and to lesser extent immediate recall subscores, and lower scores were most strongly associated with infarcts in the anterior and lateral temporal regions. Mode 4 was predominantly driven by learning ability subscores, and was associated with infarcts in left frontal regions, including the basal ganglia. The explained variances of the four canonical modes were 0.404, 0.275, 0.204, and 0.191, respectively.

We related the CCA results back to the theoretical constructs of verbal memory functions (Table 1) by evaluating whether cognitive patterns in each canonical mode fit the predefined patterns. Mode 2 corresponded with our prior construct for consolidation: strong association with impaired delayed recall and recognition, but no association with immediate recall or learning ability. Mode 4 corresponded with our construct for encoding, showing a strong association with impaired learning ability. In this mode, lack of association with other SVLT subscores can be explained as downstream effect, that is, resulting from explained variance already extracted in Modes 1 through 3, leaving learning ability as most specific score for encoding. Modes 1 and 3 did not clearly fit any of the predefined patterns. Figure S1 shows that CCA results remained essentially the same without correction for total infarct volume.

4 | DISCUSSION

This study shows how CCA can complement multivariable single-outcome LSM by taking cross-dependencies between lesion locations and cognitive scores into account. Using verbal memory functions as a proof-of-concept, multivariable single-outcome LSM alone showed that individual SVLT subscores were associated with largely overlapping locations, providing limited insight into the neural correlates of verbal memory functions. CCA revealed that cognitive patterns representative of specific verbal memory functions, specifically encoding and consolidation, were linked to distinct infarct patterns. Our findings thus demonstrate the added value of CCA in LSM to help disentangle lesion-behavior associations.

Dealing with interdependencies between cognitive tests is an important challenge in the LSM field (Sperber et al., 2020). A recent methodological study analyzed two common approaches for dealing with this issue, namely indirect comparison of parallel univariate analyses and correcting for related cognitive scores through nuisance regression. The authors found that both approaches suffer from topographical bias and false-positive artifacts (Sperber et al., 2020). Furthermore, as our SVR-ROI results illustrate, interpretation of parallel univariate analysis results is hampered by the need to select distinct and overlapping spatial results, leading to loss of information and lack of sensitivity (see Figure 5).

Using verbal memory functions as a proof of concept, we demonstrated that CCA offers a viable solution to these challenges. With CCA we identified SVLT subscore patterns extracted by the canonical modes that aligned with prior theoretical knowledge on encoding and consolidation (Lezak et al., 2012; Vanderploeg et al., 2001). The identified neuroanatomical correlates also fit with prior knowledge, thus supporting the validity of our findings. We found that cognitive test score pattern that fit encoding impairment was linked to frontal infarcts (Mode 4), which aligns with evidence from functional imaging studies that show that frontal lobes are activated during encoding processes (Budson & Price, 2009). Meanwhile, the pattern for consolidation impairment (Mode 2) was linked to medial temporal lobe infarcts, also in line with extensive literature (McGaugh, 2000; Squire & Zola-Morgan, 1991). Of note, LSM studies on verbal memory are scarce (recent review in Lugtmeijer et al., 2021), and to our knowledge none compared multiple (sub)scores. One LSM study ($N = 88$) did find that recognition score impairment on the Rey Auditory Verbal Learning Test (i.e., highly similar to the SVLT) was associated with left medial temporal lobe and temporo-occipital infarcts, which is in line with our results (Biesbroek et al., 2015).

This proof-of-concept study demonstrated the potential value of CCA as novel LSM approach. It is important to note that our study provides a single application of this approach using real-life data, and was not designed to establish method validity. As next step, validation studies are needed to establish the validity and robustness of CCA for broader use in LSM. Validation studies could be performed using simulated behavioral data, similar to previous studies (Mah et al., 2014; Sperber et al., 2020; Sperber & Karnath, 2017), to circumvent the lack of a gold standard for validation. In addition, these validation studies should address applicability in smaller sample sizes, considering that our dataset was exceptionally large compared with most available LSM studies (generally $N < 400$; Weaver et al., 2019).

Strengths of this study are the large homogenous study sample and use of well-defined cognitive functions and cognitive tests with a

10970193, 2023, 6, Downloaded from https://onlinelibrary.wiley.com/doi/10.1002/hbm.26208 by Utrecht University Library, Wiley Online Library on [11/05/2023]. See the Terms and Conditions (https://onlinelibrary.wiley.com/terms-and-conditions) on Wiley Online Library for rules of use; OA articles are governed by the applicable Creative Commons License

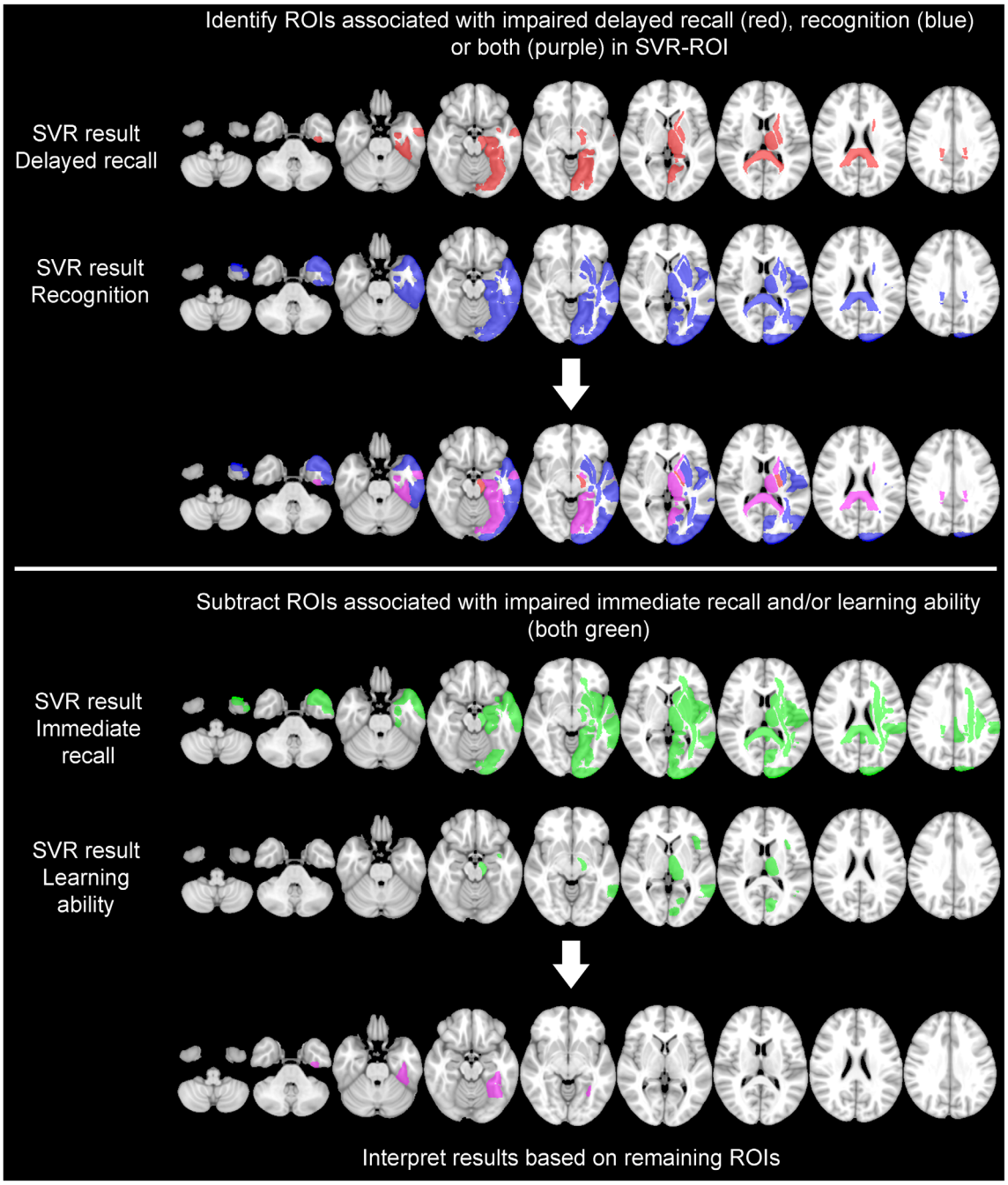

FIGURE 5 Relating support vector regression (SVR) results back to theoretical constructs of verbal memory functions. This figure illustrates how the actual SVR region of interest (ROI)-based lesion-symptom mapping (LSM [SVR-ROI]) results can be related back to the theoretical constructs of consolidation and retrieval functions through single-outcome LSM approaches. Note that the presented results are the same as in Figure 4b, but all significant ROIs per SVLT subscore are shown in a single color rather than a scale. By convention, an isolated consolidation deficit would be reflected by impairment in both delayed recall and recognition, but with relatively unimpaired immediate recall and learning ability (see definitions Table 1). Thus, we first identified ROIs associated with both delayed recall and recognition impairment (purple ROIs, upper panel). Next, ROIs associated with immediate recall and/or learning ability (green) were subtracted, resulting in only two ROIs attributed to consolidation (purple ROIs, bottom panel). Along the same lines, a specific retrieval deficit should be reflected in impaired delayed recall, but with all other subscores relatively unimpaired. Retrieval would thus be ascribed to ROIs linked to delayed recall (red ROIs, upper panel), after subtracting ROIs associated with immediate recall and/or learning ability impairment (bottom panel; green ROIs). No ROIs matched this combination. This demonstrates how this approach to interpreting single-outcome LSM results, that is, analyzing distinct and overlapping results (as shown in Figure 1), provides limited insight into the neural correlates of cognitive functions. Particularly in the subtraction step information is lost; however, this cannot be avoided without taking the relative contribution of different subscores into account.

10970193, 2023, 6, Downloaded from https://onlinelibrary.wiley.com/doi/10.1002/hbm.26208 by Utrecht University Library, Wiley Online Library on [11/05/2023]. See the Terms and Conditions (https://onlinelibrary.wiley.com/terms-and-conditions) on Wiley Online Library for rules of use; OA articles are governed by the applicable Creative Commons License

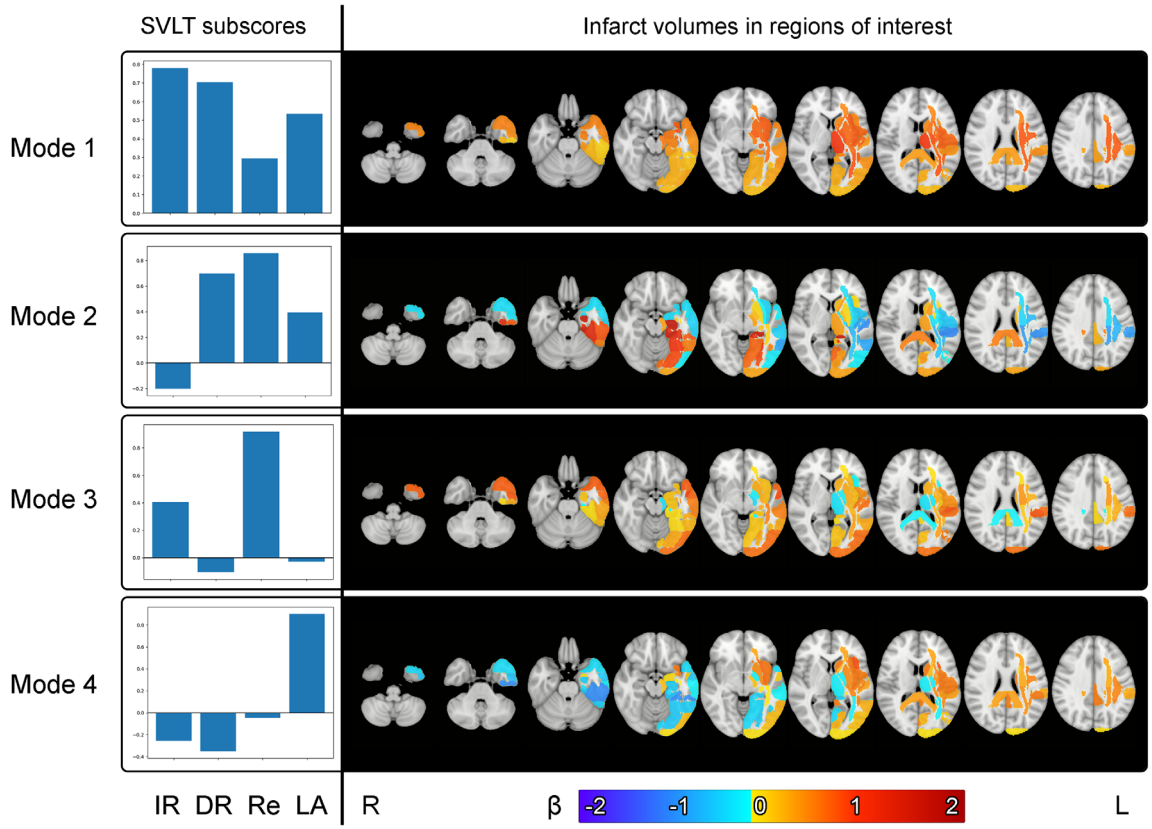

FIGURE 6 Multioutcome canonical correlation analysis results. Combined multivariable and multioutcome lesion-symptom mapping with canonical correlation analysis (CCA). Only statistically significant regions of interest (ROIs) from the SVR-ROI ($p < .05$, 5000 permutations) for one or more of the four Seoul Verbal Learning Test (SVLT) subscores were used in the CCA to reduce noise. Forty-nine ROIs and four SVLT subscores and were entered in a single model to identify the four canonical modes that each represent a unique pattern of paired test score and lesion data. Modes are extracted consecutively, that is, Mode 1 has the highest explained variance and is therefore extracted first; once this information has been extracted, Mode 2 captures the remaining variance, and so on. For each mode, positive betas on both the SVLT subscore (bar on positive y axis) and ROIs (colors yellow to red) indicate that poorer performance on the SVLT subscore(s) is linked to higher infarct volumes. Note that beta values indicate a relative contribution of all included variables in the CCA analyses, therefore neutral or negative betas indicate that these SVLT subscores and/or brain regions do not contribute to a particular mode. DR, delayed recall; IR, immediate recall; L, left.; LA, learning ability; R, right; Re, recognition

firm theoretical basis. Some potential limitations must also be noted. First, CCA is exploratory by nature, which means that it does not provide statistical significance (Wang et al., 2020). Through random permutation testing we showed that within each mode, ROIs with high betas were statistically significant ($p < 0.05$), demonstrating the robustness of our findings. Second, CCA did not allow for voxel-based analyses—which are often preferred in LSM because of the higher spatial resolution than ROI-based analyses—because of the high dimensionality that would be required. Therefore, spatial resolution of the CCA results is relatively low compared with VLSM and remains dependent on brain atlases. Third, the time interval between stroke onset and SVLT assessment was relatively wide (range 1–365 days). Brain plasticity and functional recovery can occur after stroke, and the degree of recovery may depend on which brain region is damaged. Finally, an inherent limitation of CCA is that it creates canonical modes based on positive and negative coefficients, while only positive coefficients are relevant from a clinical perspective in LSM (see Section 2). This means a form of feature selection is needed prior to CCA to minimize the impact of negative coefficients, for which we applied SVR-ROI as first step. However, this might lead to loss of information due to statistical thresholding. Further research is necessary to determine how to best incorporate CCA into LSM pipelines.

5 | CONCLUSION

We showcase the value of CCA as multivariable and multioutcome LSM approach. This approach creates a novel opportunity to address a multitude of research questions focused on disentangling complex or interrelated brain processes in relation to their neuroanatomical correlates. Like other LSM methods, this can be applied in the context of stroke for acute infarcts, but also for other lesion types (e.g., white matter hyperintensities or brain tumors). Further investigation in independent datasets using different cognitive outcome measures, possibly with simulated cognitive data, is warranted to establish the validity of CCA, for broader application in LSM studies (Bzdok & Yeo, 2017;

10970193, 2023, 6, Downloaded from https://onlinelibrary.wiley.com/doi/10.1002/hbm.26208 by Utrecht University Library, Wiley Online Library on [11/05/2023]. See the Terms and Conditions (https://onlinelibrary.wiley.com/terms-and-conditions) on Wiley Online Library for rules of use; OA articles are governed by the applicable Creative Commons License

Wang et al., 2020). Of note, this approach benefits large datasets with extensive brain coverage and availability of multiple cognitive test scores, and thus could benefit from multicenter designs through consortia such as STROKOG (Sachdev et al., 2017) and Meta-VCI-Map (Weaver et al., 2019).

ACKNOWLEDGMENTS

This work was supported by Vici grant 918.16.616 from ZonMw, The Netherlands, Organization for Health Research to Geert Jan Biessels. J. Matthijs Biesbroek was supported by a Young Talent Fellowship from the UMC Utrecht Brain. Danilo Bzdok was supported by the Brain Canada Foundation, through the Canada Brain Research Fund, with the financial support of Health Canada, National Institutes of Health (NIH R01 AG068563A, NIH R01 R01DA053301-01A1), the Canadian Institute of Health Research (CHIR) (CIHR 438531, CIHR 470425), the Healthy Brains Healthy Lives initiative (Canada First Research Excellence fund), Google (Research Award, Teaching Award), and by the CIFAR Artificial Intelligence Chairs program (Canada Institute for Advanced Research). Hugo J. Kuijf was supported by the Dutch Heart Foundation (03-004-2021-T043).

DATA AVAILABILITY STATEMENT

The data that support the findings of this study are available from the corresponding author upon reasonable request. Project data were shared between participating centers in accordance with the guidelines of the Meta-VCI-Map consortium (www.metavcimap.org; Weaver et al., 2019).

ORCID

Nick A. Weaver https://orcid.org/0000-0001-8425-8436
Jae-Sung Lim https://orcid.org/0000-0001-6157-2908
Johannes Matthijs Biesbroek https://orcid.org/0000-0001-7017-2148
Geert Jan Biessels https://orcid.org/0000-0001-6862-2496
Hee-Joon Bae https://orcid.org/0000-0003-0051-1997
Danilo Bzdok https://orcid.org/0000-0003-3466-6620
Hugo J. Kuijf https://orcid.org/0000-0001-6997-9059

REFERENCES

Abraham, A., Pedregosa, F., Eickenberg, M., Gervais, P., Mueller, A., Kossaifi, J., Gramfort, A., Thirion, B., & Varoquaux, G. (2014). Machine learning for neuroimaging with scikit-learn. *Frontiers in Neuroinformatics*, *8*, 14.

Baddeley, A. D., & Hitch, G. (1974). Working memory. *Psychology of Learning and Motivation – Advances in Research Theory*, *8*, 47–89.

Bates, E., Wilson, S. M., Saygin, A. P., Dick, F., Sereno, M. I., Knight, R. T., & Dronker, N. F. (2003). Voxel-based lesion-symptom mapping. *Nature Neuroscience*, *6*, 448–450.

Biesbroek, J. M., Kuijf, H. J., Weaver, N. A., Zhao, L., Duering, M., & Biessels, G. J. (2019). Brain infarct segmentation and registration on MRI or CT for lesion-symptom mapping. *Journal of Visualized Experiments*, e59653.

Biesbroek, J. M., Lim, J. S., Weaver, N. A., Arikan, G., Kang, Y., Kim, B. J., Kuijf, H. J., Postma, A., Lee, B. C., Lee, K. J., Yu, K. H., Bae, H. J., & Biessels, G. J. (2021). Anatomy of phonemic and semantic fluency: A lesion and disconnectome study in 1231 stroke patients. *Cortex*, *143*, 148–163.

Biesbroek, J. M., van Zandvoort, M. J. E., Kappelle, L. J., Schoo, L., Kuijf, H. J., Velthuis, B. K., Biessels, G. J., & Postma, A. (2015). Distinct anatomical correlates of discriminability and criterion setting in verbal recognition memory revealed by lesion-symptom mapping. *Human Brain Mapping*, *36*, 1292–1303.

Biesbroek, J. M., van Zandvoort, M. J. E., Kappelle, L. J., Velthuis, B. K., Biessels, G. J., & Postma, A. (2016). Shared and distinct anatomical correlates of semantic and phonemic fluency revealed by lesion-symptom mapping in patients with ischemic stroke. *Brain Structure & Function*, *221*, 2123–2134.

Budson, A. E., & Price, B. H. (2009). Memory dysfunction. *The New England Journal of Medicine*, *352*, 692–699. https://doi.org/10.1056/NEJMra041071

Bzdok, D., Nichols, T. E., & Smith, S. M. (2019). Towards algorithmic analytics for large-scale datasets. *Nature Machine Intelligence*, *1*, 296–306.

Bzdok, D., & Yeo, B. T. T. (2017). Inference in the age of big data: Future perspectives on neuroscience. *NeuroImage*, *155*, 549–564.

Clemens, B., Derntl, B., Smith, E., Junger, J., Neulen, J., Mingoia, G., Schneider, F., Abel, T., Bzdok, D., & Habel, U. (2020). Predictive pattern classification can distinguish gender identity subtypes from behavior and brain imaging. *Cerebral Cortex*, *30*, 2755–2765.

de Haan, B., & Karnath, H. O. (2017). A Hitchhiker's guide to lesion-behaviour mapping. *Neuropsychologia*, *115*, 5–16. https://doi.org/10.1016/j.neuropsychologia.2017.10.021

Fonov, V., Evans, A. C., Botteron, K., Almli, C. R., McKinstry, R. C., Collins, D. L., & Brain Development Cooperative Group. (2011). Unbiased average age-appropriate atlases for pediatric studies. *NeuroImage*, *54*, 313–327.

Hammers, A., Allom, R., Koepp, M. J., Free, S. L., Myers, R., Lemieux, L., Mitchell, T. N., Brooks, D. J., & Duncan, J. S. (2003). Three-dimensional maximum probability atlas of the human brain, with particular reference to the temporal lobe. *Human Brain Mapping*, *19*, 224–247.

Hotelling, H. (1936). Relations between two sets of variates. *Biometrika*, *28*, 321–377.

Kang, Y., & Na, D. (2003). *Seoul neuropsychological screening battery (SNSB)*. Incheon Human Brain Research & Consulting Co.

Karnath, H. O., Sperber, C., & Rorden, C. (2018). Mapping human brain lesions and their functional consequences. *NeuroImage*, *165*, 180–189. https://doi.org/10.1016/j.neuroimage.2017.10.028

Lezak, M. D., Howieson, D. B., Bigler, E. D., & Tranel, D. (2012). *Neuropsychological assessment* (5th ed.). Oxford University Press.

Lim, J., Kim, N., Jang, M. U., Han, M., Kim, S., Baek, M. J., Lee, J. S., Lee, J., Lee, B., & Yu, K. (2014). Cortical hubs and subcortical cholinergic pathways as neural substrates of poststroke dementia. *Stroke*, *45*(4), 1069–1076.

Lugtmeijer, S., Lammers, N. A., de Haan, E. H. F., de Leeuw, F. E., & Kessels, R. P. C. (2021). Post-stroke working memory dysfunction: A meta-analysis and systematic review. *Neuropsychology Review*, *31*, 202–219.

Mah, Y. H., Husain, M., Rees, G., & Nachev, P. (2014). Human brain lesion-deficit inference remapped. *Brain*, *137*, 2522–2531.

Makris, N., Goldstein, J. M., Kennedy, D., Hodge, S. M., Caviness, V. S., Faraone, S. V., Tsuang, M. T., & Seidman, L. J. (2006). Decreased volume of left and total anterior insular lobule in schizophrenia. *Schizophrenia Research*, *83*, 155–171.

McGaugh, J. L. (2000). Memory--a century of consolidation. *Science*, *287*, 248–251. https://doi.org/10.1126/science.287.5451.248

Mirman, D., Landrigan, J. F., Kokolis, S., Verillo, S., Ferrara, C., & Pustina, D. (2017). Corrections for multiple comparisons in voxel-based lesion-symptom mapping. *Neuropsychologia*, *115*, 112–123. https://doi.org/10.1016/j.neuropsychologia.2017.08.025

Mori, S., Oishi, K., Jiang, H., Jiang, L., Li, X., Akhter, K., Hua, K., Faria, A. V., Mahmood, A., Woods, R., Toga, A. W., Pike, G. B., Neto, P. R., Evans, A., Zhang, J., Huang, H., Miller, M. I., van Zijl, P., & Mazziotta, J. (2008). Stereotaxic white matter atlas based on diffusion tensor imaging in an ICBM template. *NeuroImage*, *40*, 570–582.

10970193, 2023, 6, Downloaded from https://onlinelibrary.wiley.com/doi/10.1002/hbm.26208 by Utrecht University Library, Wiley Online Library on [11/05/2023]. See the Terms and Conditions (https://onlinelibrary.wiley.com/terms-and-conditions) on Wiley Online Library for rules of use; OA articles are governed by the applicable Creative Commons License

Pedregosa, F., Varoquaux, G., Gramfort, A., Michel, V., Thirion, B., Grisel, O., Blondel, M., Prettenhofer, P., Weiss, R., Dubourg, V., Vanderplas, J., Passos, A., Cournapeau, D., Brucher, M., Perrot, M., & Duchesnay, É. (2011). Scikit-learn: Machine learning in python. *Journal of Machine Learning Research*, *12*, 2825–2830.

Pustina, D., Avants, B., Faseyitan, O. K., Medaglia, J. D., & Coslett, H. B. (2017). Improved accuracy of lesion to symptom mapping with multivariate sparse canonical correlations. *Neuropsychologia*, *115*, 154–166. https://doi.org/10.1016/j.neuropsychologia.2017.08.027

Ritter, F., Boskamp, T., Homeyer, A., Laue, H., Schwier, M., Link, F., & Peitgen, H. (2011). Medical image analysis. *IEEE Pulse*, *2*, 60–70.

Rorden, C., & Karnath, H. O. (2004). Using human brain lesions to infer function: A relic from a past era in the fMRI age? *Nature Reviews. Neuroscience*, *5*, 812–819.

Rorden, C., Karnath, H. O., & Bonilha, L. (2007). Improving lesion-symptom mapping. *Journal of Cognitive Neuroscience*, *19*, 1081–1088.

Sachdev, P. S., Lo, J. W., Crawford, J. D., Mellon, L., Hickey, A., Williams, D., Bordet, R., Mendyk, A. M., Gelé, P., Deplanque, D., Bae, H. J., Lim, J. S., Brodtmann, A., Werden, E., Cumming, T., K €ohler, S., Verhey, F. R. J., Dong, Y. H., Tan, H. H., … Kochan, N. A. (2017). STROKOG (stroke and cognition consortium): An international consortium to examine the epidemiology, diagnosis, and treatment of neurocognitive disorders in relation to cerebrovascular disease. *Alzheimer's Dement Diagnosis, Assessment & Disease Monitoring*, *7*, 11–23.

Sperber, C., & Karnath, H. O. (2017). On the validity of lesion-behaviour mapping methods. *Neuropsychologia*, *115*, 17–24. https://doi.org/10.1016/j.neuropsychologia.2017.07.035

Sperber, C., Nolingberg, C., & Karnath, H.-O. (2020). Post-stroke cognitive deficits rarely come alone: Handling co-morbidity in lesion-behaviour mapping. *Human Brain Mapping*, *41*, 1387–1399. https://doi.org/10.1002/hbm.24885

Squire, L. R., & Zola-Morgan, S. (1991). The medial temporal lobe memory system. *Science*, *253*, 1380–1386.

Vanderploeg, R. D., Crowell, T. A., & Curtiss, G. (2001). Verbal learning and memory deficits in traumatic brain injury: Encoding, consolidation, and retrieval. *Journal of Clinical and Experimental Neuropsychology*, *23*, 185–195.

Wang, H. T., Smallwood, J., Mourao-Miranda, J., Xia, C. H., Satterthwaite, T. D., Bassett, D. S., & Bzdok, D. (2020). Finding the needle in a high-dimensional haystack: Canonical correlation analysis for neuroscientists. *NeuroImage*, *216*, 116745.

Weaver, N. A., Kancheva, A. K., Lim, J.-S., Biesbroek, J. M., Wajer, I. M. H., Kang, Y., Kim, B. J., Kuijf, H. J., Lee, B.-C., Lee, K.-J., Yu, K.-H., Biessels, G. J., & Bae, H.-J. (2021). Post-stroke cognitive impairment on the mini-mental state examination primarily relates to left middle cerebral artery infarcts. *International Journal Stroke*, *16*, 981–989. https://doi.org/10.1177/1747493020984552

Weaver, N. A., Zhao, L., Biesbroek, J. M., Kuijf, H. J., Aben, H. P., Bae, H.-J., Caballero, M. Á. A., Chappell, F. M., Chen, C. P. L. H., Dichgans, M., Duering, M., Georgakis, M. K., van der Giessen, R. S., Gyanwali, B., Hamilton, O. K. L., Hilal, S., vom Hofe, E. M., de Kort, P. L. M., Koudstaal, P. J., … Biessels, G. J. (2019). The meta VCI map consortium for meta-analyses on strategic lesion locations for vascular cognitive impairment using lesion-symptom mapping: Design and multicenter pilot study. *Alzheimer's Dement Diagnosis, Assessment & Disease Monitoring*, *11*, 310–326.

Wilson, S. M., Henry, M. L., Besbris, M., Ogar, J. M., Dronkers, N. F., Jarrold, W., Miller, B. L., & Gorno-Tempini, M. L. (2010). Connected speech production in three variants of primary progressive aphasia. *Brain*, *133*, 2069–2088.

Yourganov, G., Fridriksson, J., Rorden, C., Gleichgerrcht, E., & Bonilha, L. (2016). Multivariate connectome-based symptom mapping in post-stroke patients: Networks supporting language and speech. *The Journal of Neuroscience*, *36*, 6668–6679.

Yu, K. H., Cho, S. J., Oh, M. S., Jung, S., Lee, J. H., Shin, J. H., Koh, I. S., Cha, J. K., Park, J. M., Bae, H. J., Kang, Y., & Lee, B. C. (2013). Cognitive impairment evaluated with vascular cognitive impairment harmonization standards in a multicenter prospective stroke cohort in Korea. *Stroke*, *44*, 786–788. https://doi.org/10.1161/STROKEAHA.112.668343

Zhang, Y., Kimberg, D. Y., Coslett, H. B., Schwartz, M. F., & Wang, Z. (2014). Multivariate lesion-symptom mapping using support vector regression. *Human Brain Mapping*, *35*, 5861–5876.

Zhao, L., Biesbroek, J. M., Shi, L., Liu, W., Kuijf, H. J., Chu, W. W. C., Abrigo, J. M., Lee, R. K. L., Leung, T. W. H., Lau, A. Y. L., Biessels, G. J., Mok, V., & Wong, A. (2017). Strategic infarct location for post-stroke cognitive impairment: A multivariate lesion-symptom mapping study. *Journal of Cerebral Blood Flow and Metabolism*, *38*, 1299–1311.

SUPPORTING INFORMATION

Additional supporting information can be found online in the Supporting Information section at the end of this article.

How to cite this article: Weaver, N. A., Mamdani, M. H., Lim, J.-S., Biesbroek, J. M., Biessels, G. J., Huenges Wajer, I. M. C., Kang, Y., Kim, B. J., Lee, B.-C., Lee, K.-J., Yu, K.-H., Bae, H.-J., Bzdok, D., & Kuijf, H. J. (2023). Disentangling poststroke cognitive deficits and their neuroanatomical correlates through combined multivariable and multioutcome lesion-symptom mapping. *Human Brain Mapping*, *44*(6), 2266–2278. https://doi.org/10.1002/hbm.26208

10970193, 2023, 6, Downloaded from https://onlinelibrary.wiley.com/doi/10.1002/hbm.26208 by Utrecht University Library, Wiley Online Library on [11/05/2023]. See the Terms and Conditions (https://onlinelibrary.wiley.com/terms-and-conditions) on Wiley Online Library for rules of use; OA articles are governed by the applicable Creative Commons License